

Article

Lytic Polysaccharide Monooxygenases from *Serpula lacrymans* as Enzyme Cocktail Additive for Efficient Lignocellulose Degradation

Fei Li ^{1,†} , Yang Liu ^{2,†}, Honglu Zhao ², Xuan Liu ² and Hongbo Yu ^{2,*} 

¹ Department of Bioengineering, School of Chemistry and Chemical Engineering, Wuhan University of Science and Technology, Wuhan 430081, China; biolifei@wust.edu.cn

² Department of Biotechnology, College of Life Science and Technology, Huazhong University of Science and Technology, Wuhan 430074, China; m202071962@hust.edu.cn (Y.L.); izhaohonglu@163.com (H.Z.); m201771708@hust.edu.cn (X.L.)

* Correspondence: yuhongbo@hust.edu.cn

† These authors contributed equally to this work and share first authorship.

Abstract: Lytic polysaccharide monooxygenase (LPMO) could oxidize and cleavage the glycosidic bonds of polysaccharides in lignocellulose, thereby promoting the hydrolysis of polysaccharide substrates by glycoside hydrolases and significantly improving the saccharification efficiency of lignocellulose. Brown-rot fungi are typical degraders of lignocellulose and contain multiple LPMO genes of the AA14 family and AA9 family, however, the AA14 LPMO from brown-rot fungi was rarely reported. Herein, the transcriptomic analysis of *Serpula lacrymans* incubated in the presence of pine exhibited that an AA14 LPMO (*S/LPMO14A*) was significantly upregulated and there were redox interactions between LPMOs and other enzymes (AA3, AA6, and hemicellulose degrading enzyme), indicating that *S/LPMO14A* may be involved in the degradation of polysaccharides. Enzymatic profiling of *S/LPMO14A* showed the optimal pH of 8.0 and temperature of 50 °C and it had higher reaction activity in the presence of 40% glycerol and acetonitrile. *S/LPMO14A* could significantly improve the saccharification of pine and xylan-coated cellulose substrate to release glucose and xylose by cellulase and xylanase by disturbing the surface structure of lignocellulose based on environmental scanning electron microscope and atomic force microscopy analysis.

Keywords: LPMO; *Serpula lacrymans*; lignocellulose degradation; saccharification



Citation: Li, F.; Liu, Y.; Zhao, H.; Liu, X.; Yu, H. Lytic Polysaccharide Monooxygenases from *Serpula lacrymans* as Enzyme Cocktail Additive for Efficient Lignocellulose Degradation. *Fermentation* **2023**, *9*, 506. <https://doi.org/10.3390/fermentation9060506>

Academic Editor: Mohammad Taherzadeh

Received: 16 April 2023

Revised: 23 May 2023

Accepted: 23 May 2023

Published: 24 May 2023



Copyright: © 2023 by the authors. Licensee MDPI, Basel, Switzerland. This article is an open access article distributed under the terms and conditions of the Creative Commons Attribution (CC BY) license (<https://creativecommons.org/licenses/by/4.0/>).

1. Introduction

Lignocellulose is the most abundant renewable resource in nature, which provides a sustainable substitute for fossil fuels, and has a wide application potential in the field of biorefinery. The discovery of lytic polysaccharide monooxygenases (LPMO) was of great significance for the degradation of polysaccharides in lignocellulose [1,2]. LPMO can oxidize and break the glycosidic bonds of polysaccharides such as cellulose, chitin, and starch, thereby reducing the resistance of polysaccharide conversion and promoting the hydrolysis of polysaccharide substrates by glycoside hydrolases [3]. LPMOs have abundant structural and substrate diversity, indicating that LPMOs could play diverse functions in nature [4,5].

Brown-rot fungi are the most important wood-rot basidiomycetes in the coniferous forest ecosystem and have a unique low-energy-consumption strategy to depolymerize lignocellulose. Brown-rot fungi have evolved a two-step biodegradation mechanism of lignocellulose. Lignocellulose is first oxidized by hydroxyl radicals generated by extracellular Fenton reaction ($\text{H}_2\text{O}_2 + \text{Fe}^{2+} \rightarrow \bullet\text{OH} + \text{OH}^- + \text{Fe}^{3+}$) to depolymerize or modify lignin in the early stage, and subsequently, the exposed polysaccharide is oxidized as an absorbable carbon source by limited glycoside hydrolase in the later stage [6,7]. Brown-rot fungi preferentially degrade hemicellulose to disrupt the long-chain polymeric nature of the cell wall carbohydrates in the early decay process of brown-rot fungi [8]. Brown-rot fungi contain

multiple LPMO genes related to the degradation of lignocellulosic polysaccharides, mainly belonging to two families of auxiliary activity (AAs) in the carbohydrate-active enzymes (CAZy): AA9 and AA14 [9–11], responsible for the degradation of cellulose and xylan respectively. A study has found that when *S. lacrymans* grows on lignocellulose as a carbon source, the LPMO genes are significantly upregulated (defined as the GH61 family at the time) [12]. Kojima et al. reported AA9 LPMOs could decrease wood strength in the early stage of brown-rot fungi wood decay by depolymerizing the backbone of xyloglucan [13]. AA9 has been widely studied and reported in promoting cellulose hydrolysis, but AA14 is less studied.

Unlike AA9, which cleaves the glycosidic bonds in crystalline cellulose, AA14 enhances biomass degradation by oxidatively breaking the bond of xylan-coated cellulose fibers. Couturier et al. [14] and Zerva et al. identified [15] a significant synergistic interaction between AA14s from white-rot fungus and an enzyme cocktail and xylanase for lignocellulose degradation, respectively. Mahajan et al. [16] also reported that two AA14 LPMOs and one pyrroloquin-olinequinone-dependent oxidoreductase (AA12) contributed to the lignocellulosic plant biomass degradation according to the transcriptomic analysis of the white-rot fungus *Podocorypha petalodes* GGF6, but enzymatic hydrolysis characteristics of the two AA14 LPMOs are not clear. There are few studies on the role of AA14 LPMOs in the degradation of lignocellulose by brown-rot fungi. The characteristics of AA14 from the brown-rot fungus and its enzymatic saccharification for biomass were rarely reported.

In this study, we analyzed the transcriptome of *S. lacrymans* cultured on lignocellulose to reveal the expression pattern of carbohydrate-degrading enzymes and auxiliary enzymes, which showed that the *SILPMO14A* could contribute to polysaccharides degradation. The biochemical characteristics of *SILPMO14A* were studied. Saccharification of pine and xylan-coated cellulose substrate in the presence of *SILPMO14A* was performed. This study contributes to further understanding the role of AA14 in wood decay by brown-rot fungi and lays a foundation for its application in the field of biorefinery.

2. Materials and Methods

2.1. Strains and Medium

Serpula lacrymans (Wulfen) Schroeter NBRC 30955 (*S. lacrymans*) was preserved in our laboratory and stored at 4 °C. The strain was inoculated on MEA solid medium (3% malt extract, 0.3% soy peptone, and 1.5% agar) for cultivation at 20 °C. *Escherichia coli* Rosetta (DE3) was used for gene cloning and expression of *SILPMO14A*.

2.2. Transcriptome Analysis of *Serpula Lacrymans* Incubated on Pine

S. lacrymans was inoculated into MEA liquid medium (3% malt extract and 0.3% soy peptone) under 180 rpm for 5 days at 20 °C, then the mycelial homogenate was inoculated into solid medium containing 1 g of pine (substrate: MEA = 1:20) in 250 mL flasks and grown at 20 °C for 30 d. The total fungal RNA was extracted using a Tiangen polysaccharide polyphenol Plant Total RNA Extraction kit (TIANGEN, Beijing, China) and sequenced using the illumina NovaSeq 6000 (illumina, San Diego, CA, USA) by Novogene (Beijing, China). RNA-seq data were spliced using Trinity and mapped to the reference genome of *S. lacrymans* S7.9 using the HISAT2 software package. Nr (diamond v0.8.22), Nt (NCBI blast 2.2.28+), Pfam (HMMER 3.0 package, hmmscan), KOG/COG (diamond v0.8.22), Swiss-prot (diamond v0.8.22), KEGG (KAAS, KEGG Automatic Annotation Server, <http://www.genome.jp/tools/kaas/>, accessed on 20 March 2022), GO (Blast2GO v2.5) and CAZy databases (dbCAN, <http://bcb.unl.edu/dbCAN2/>, accessed on 28 March 2022) were used for gene function annotation of transcriptome.

2.3. Sequence Alignment and Phylogenetic Tree Analysis of *SILPMO14A*

For sequence alignment, multiple sequence alignment for *SILPMO14A* was carried out using NCBI-BLAST (<https://blast.ncbi.nlm.nih.gov/Blast.cgi>, accessed on 5 May 2022).

Based on the sequence alignment, a phylogenetic tree was constructed with MEGA-X software according to the neighbor-joining method.

2.4. Expression and Purification of Recombinant SILPMO14A

The total RNA of *S. lacrymans* was extracted using an RNA extraction kit (TaKaRa, Dalian, China, MiniBEST Universal RNA Extraction Kit) and cDNA synthesis was performed using a cDNA synthesis kit (PrimeScript™ 1st Strand cDNA Synthesis Kit) with total RNA as a template. The obtained cDNA gene was used to amplify the target gene *SILPMO14A* by PCR (Supplementary Table S1). The PCR product of *SILPMO14A* was cloned into the modified pET-28a(+) vector with a factor Xa cleavage site. The construction of plasmid pET28a-*SILPMO14A* was referred to the method reported by Forsberg et al. [17,18]. The successfully sequenced recombinant plasmids were transformed into *E. coli* Rosetta (DE3) competent cells. Transformants were selected on LB plates containing 30 µg/mL kanamycin sulfate. The recombinant *E. coli* was cultivated and induced with 1 mM IPTG for LPMO expression.

The bacterial cells were collected via centrifugation at 12,000× *g* for 5 min and mixed with pre-cooled buffer (contained 50 mM pH 7.9 Tris-HCl, 10 mM EDTA, 5 mM DTT). The bacterial cells were lysed by a high pressure homogenizer. The inclusion bodies were collected via centrifugation at 12,000× *g* for 30 min and washed twice with inclusion body washing buffer (20 mM pH 7.9 Tris-HCl, 2 M urea, 1 mM EDTA, 5 mM DTT) and dissolved for 1 h by adding a low-concentration imidazole buffer (20 mM pH 7.9 Tris-HCl, 8 M urea, 5 mM imidazole, 0.5 M NaCl). The dissolved *SILPMO14A* was purified by Ni-Agarose Resin affinity chromatography. The purified *SILPMO14A* with final concentration of 0.1 mg/mL was refolded with 0.7 mM GSSG, 0.1 mM DTT and 500 µM CuCl₂ in 50 mM Tris-HCl buffer (pH = 9.5) for 16 h at 4 °C in the dark. The supernatants containing the active protein were collected via centrifugation at 12,000× *g* for 10 min, and further concentrated and dialyzed in 20 mM Tris-HCl buffer (pH = 7.4). In order to avoid the influence of His-tag and copper ions on the experiment, a Factor Xa Cleavage Capture Kit (Novagen, Madison, WI, USA) was used to cleave the His-tag, and excess copper ions were removed through a PD MidiTrap G-25 desalting column (GE Healthcare, Chicago, IL, USA) [17,19]. The activities of *SILPMO14A* were detected by the Amplex Red Assay/horseradish peroxidase assay [20].

2.5. Enzymatic Properties of SILPMO14A

The enzymatic properties of *SILPMO14A* were studied using the reported oxidation reaction of 2,6-dimethoxyphenol (DMP) by LPMO [21]. For the effect of temperature on the activity of *SILPMO14A*, the reaction included 100 mM pH 8.0 Tris-HCl buffer, 1 mM DMP, 2 µM *SILPMO14A*, and 100 µM H₂O₂. The reaction was carried out at 30~80 °C. The enzyme activity was calculated by measuring the change of absorbance value at 469 nm, and the highest enzyme activity was set as 100%. In order to evaluate the effect of temperature on the stability of *SILPMO14A*, *SILPMO14A* was incubated for 0, 1, 2, and 4 h at 30~70 °C, then, samples were taken to determine the enzyme activity at room temperature, and the initial enzyme activity was set as 100%.

For the effect of pH on the activity of *SILPMO14A*, the reaction included 1 mM DMP, 2 µM *SILPMO14A*, and 100 µM H₂O₂ in Britton-Robinson buffer (pH 4~9). The change of absorbance was measured at 469 nm, and the highest enzyme activity was set as 100%. In order to determine the effect of pH on the stability of *SILPMO14A*, *SILPMO14A* was incubated for 2 and 6 h at pH 6~9, then sampled to determine the residual enzyme activity, and the enzyme activity of *SILPMO14A* without treatment was set as 100%.

To determine the effect of organic reagents on the activity of *SILPMO14A*, the reaction included 100 mM pH 7.0 Tris-HCl buffer, 5~40% of different organic reagents (methanol, ethanol, DMSO, glycerol, acetonitrile, and ethylene glycol), 1 mM DMP, 2 µM *SILPMO14A*, and 100 µM H₂O₂. The enzyme activity was calculated by measuring the change of absorbance value at 469 nm. In order to determine the effect of organic reagents on the

stability of SILPMO14A, SILPMO14A was incubated with 10% and 40% of different organic reagent for 3 h. Then, the samples, after treatment with organic reagents, were taken to determine the residual enzyme activity, and the enzyme activity of SILPMO14A without treatment was set as 100%.

2.6. Polysaccharides Cleavage, ESEM and AFM Analysis

The reaction mixture for SILPMO14A activity contained 10 mg/mL acid pretreated pine substrate [22] and xylan-coated cellulose film prepared according to Ni H.'s method [23], 1 mM ascorbic acid, 1 μ M SILPMO14A in 50 mM sodium acetate buffer (pH = 5.0), and was treated at 50 °C for 48 h. Then, the reaction mixture was purified and subjected to MALDI-TOF/TOF MS analysis [14,24]. The acid pretreated pine substrate treated by SILPMO14A was dried and subjected to environmental scanning electron microscope (ESEM, Quanta 200, FEI, Holland) analysis. To observe the morphological changes of the acid pretreated pine before and after treated by SILPMO14A, the samples were treated with gold spray, and ESEM analysis was performed at an accelerating voltage of 20.0 kV. The xylan-coated cellulose film treated by SILPMO14A was dried and subjected to atomic force microscopy (AFM) analysis [23].

2.7. Saccharification Assays

The reaction mixture for saccharification assays contained 5 mg/mL of acid pretreated pine or xylan-coated cellulose film, 1 μ M SILPMO14A, 60 FPU/(g substrates) commercial cellulase or xylanase, and 1 mM ascorbic acid in 50 mM sodium acetate buffer (pH 5.0) and were incubated at 50 °C for 24 h. The control group was treated in the absence of SILPMO14A. The sugar content was determined by HPLC using glucose and xylose as a standard, respectively [25].

3. Results and Discussion

3.1. Transcriptomic Analysis Reveals Co-Regulation of SILPMO14A with the Genes Involved in Fenton Reaction and Polysaccharides Degradation in *S. lacrymans*

To find out the key enzymes involved in lignocellulose degradation, the transcriptome samples of *S. lacrymans* grown on pine at week 2 and week 4 were analyzed (Figure 1).

A total of 39 expressed auxiliary activity proteins (AA family) were found based on the CAZy database (Figure 1A). In the early stage (2 weeks), two AA1 families (362730, 353950) involved in lignin degradation were upregulated, among which, AA1 (362730) had the higher abundant transcripts. The expression of H₂O₂-generating enzymes was also significantly upregulated, such as the AA3, AA5, and AA7 families. Of these, four AA3 family encoding genes (439506, 471949, 491425, 491377) were the most abundant transcripts, suggesting that these AA3 families might play dominant roles in H₂O₂ generation. Simultaneously, the relative abundance of 1,4-Benzoquinone reductase (AA6) (491411) was increased. Benzoquinone reductases could participate in the Fenton reaction by reducing quinones into hydroquinones, which are related to iron reductants. It is worth noting that three lytic polysaccharide monooxygenases, a recognized oxidoreductase related to polysaccharide cleavage, were upregulated, including one AA14 (468766) (SILPMO14A) and two AA9s (478045, 478044). Of these, the expression abundance of AA14 is higher than that of AA9. Some studies reported the degradation product of lignin by laccase (AA1) could serve as the electron donor source for driving the catalytic activity of LPMO [26]. SILPMO14A showed similar expression patterns and levels with the AA3 and AA6 proteins mentioned above, indicating interactions between AA3 and AA6 and AA14. Some studies have also reported that the AA6 family (quinone reductase) and AA3 family (glucose oxidase, alcohol oxidase, aryl alcohol oxidase) may be involved in the chemical process of Fenton to supply hydrogen peroxide and hydroquinones [6,27,28], which could be a co-substrate and serve as the electron donor source for achieving the catalytic activity of LPMOs [29,30].

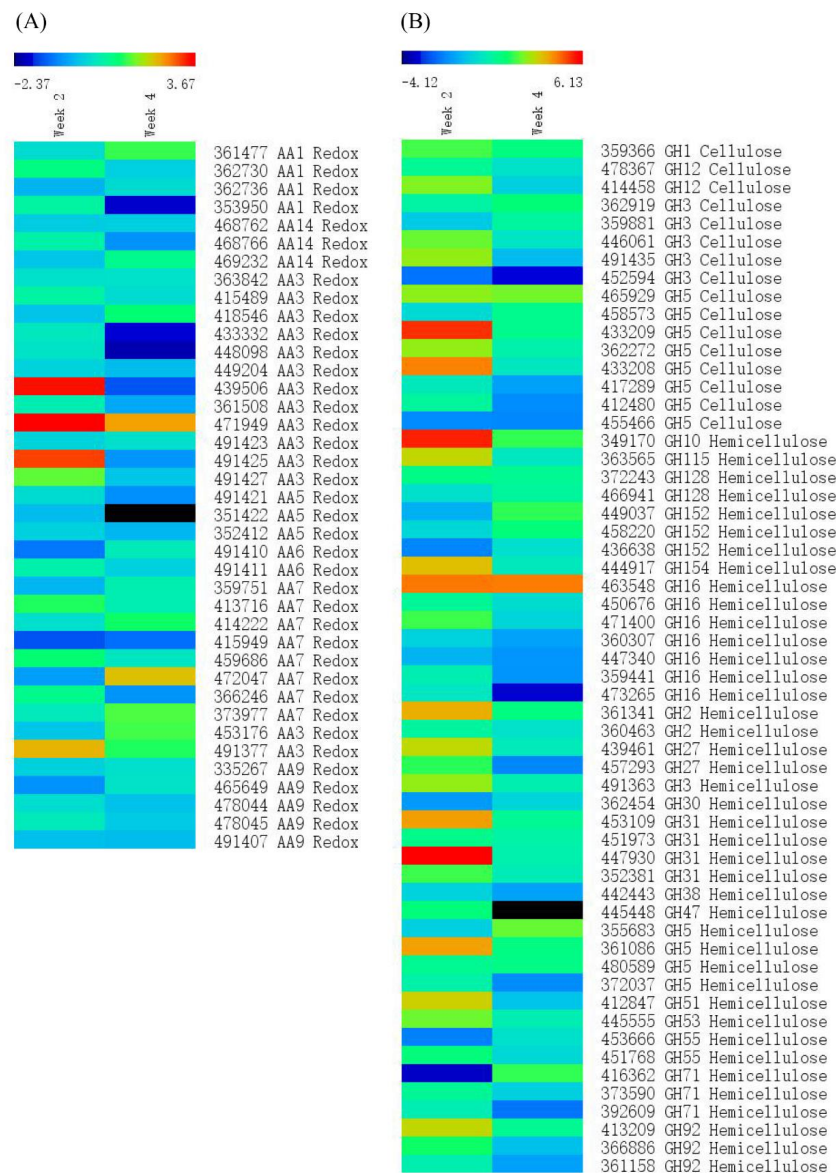


Figure 1. Transcriptome analysis of *S. lacrymans*. *S. lacrymans* was cultured for two and four weeks in the medium mixed with pine wood chips. (A) Differential gene expression of auxiliary activity families (AA) in different periods. (B) Differential gene expression of the GH family in different periods. Week 2, Week 4 represent the copy number of genes cultured on pine compared to the gene copy number cultured on MEA. Redox, cellulose and hemicellulose represented the category of redox gene in AAs, cellulose degradation and hemicellulose degradation, respectively.

The expression of the GH family genes related to cellulose and hemicellulose degradation was analyzed (Figure 1B). The total abundance of polysaccharide-degrading enzymes was higher in the early stage (week 2) than in the later stage (week 4). It can be seen that thirteen genes related to cellulose degradation were upregulated in the early stage, belonging to β -glucosidase (one GH1, three GH3, and two GH5), and endoglucanase (five GH5, two GH12). Thirty-one genes related to hemicellulose degradation were upregulated, and these hemicellulose degradation-related genes were distributed in nine glycoside hydrolase families (GH10, GH3, GH31, GH2, GH47, GH5, GH92, GH16, and GH71). Of these, the expression of the cellulose-degrading enzyme from the GH5 family (433209), and hemicellulose-degrading enzymes from the GH10 family (349170 and 447930) were the most significant. Compared with the genes related to cellulose degradation, more

genes related to hemicellulose degradation were up-expressed. This may be related to the preferential degradation of hemicellulose by brown-rot fungi in the early stage [8].

It is worth noting that the AA14 family is reported to promote the degradation of lignocellulose and increase the efficiency of wood saccharification through oxidative cleavage of the xylan-coated cellulose fibers [14]. The AA14 (468766) gene was significantly upregulated in the early stages and showed co-regulation with AA3 and AA6 redox enzymes and hemicellulose degradation-related genes when cultivating on pine wood, which indicated that it could be involved in oxidative mechanisms of polysaccharides in *S. lacrymans* and the cooperative interactions between AA3 and AA6 redox enzymes and LPMOs might be an indispensable part for the oxidative biomass degradation in wood decay by brown-rot fungi.

3.2. The Expression of *SILPMO14A* and Enzymatic Properties of *SILPMO14A*

In order to explore the role of AA14 from *S. lacrymans* in the polysaccharides' oxidation, the upregulated *SILPMO14A* (AA14, 468766) in the early stage of lignocellulose degradation by *S. lacrymans* was analyzed phylogenetically and successfully expressed in *E. coli*. The sequence blast and phylogenetic tree showed that *SILPMO14A* had a high sequence similarity with the sequence from *Leucogyrophana mollusca* (68.2%, KAH7925687.1) and was the closest neighbor with *Leucogyrophana mollusca* (Figure 2A); however, belonging to different branches and away from the branches of white-rot fungus AA14, which indicated the *SILPMO14A* was novel. After purification, SDS-PAGE showed a molecular weight of approximately 49 kDa for *SILPMO14A* (Figure 2B).

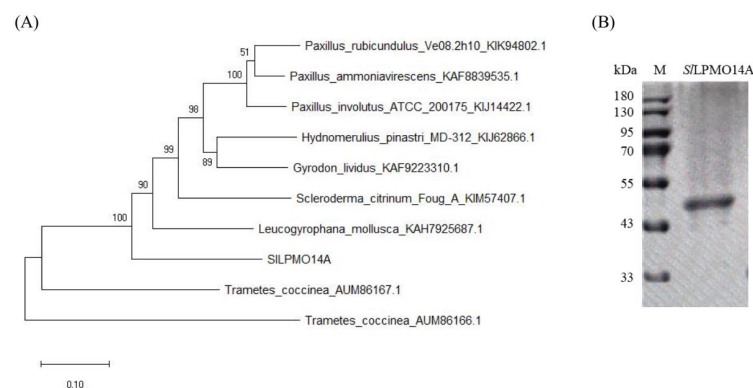


Figure 2. Phylogenetic tree construction of *SILPMO14A* and purification of *SILPMO14A*. (A) Phylogenetic tree construction of *SILPMO14A* and the other LPMO14s. (B) SDS-PAGE analysis of *SILPMO14A*.

The enzymatic properties of *SILPMO14A* were characterized (Figure 3). The results showed that *SILPMO14A* had the highest enzyme activity at 50 °C (Figure 3A), which displayed a similar optimum temperature with that of most fungal lignocellulose degrading enzymes or commercial cellulases. The highest enzyme activity with 4 U/L at 50 °C was set as 100%. The results showed over 70% of relative activity even at 80 °C (Figure 3A). The residual *SILPMO14A* activity was further detected after incubation at different temperatures for different times, and it was found that *SILPMO14A* exhibited a stable activity at 30–50 °C, and the activity loss was less when incubated for 2 h. The activity still maintained more than 70% activity of the initial *SILPMO14A* activity after 6 h incubation at 70 °C (Figure 3B), indicating that *SILPMO14A* had a good thermostability. *SILPMO14A* had the maximum enzyme activity at pH 8.0 (Figure 3C). The stability of *SILPMO14A* was better at alkaline pH than at acidic conditions. About 50% of residual activity was determined when incubated at pH 8.0 and 9.0 for 6 h, however, only retained 33.7% of the initial activity after incubation at pH 6.0 for 6 h (Figure 3D). Different organic solvents also had a certain effect on the activity and stability of enzymes, the addition of different concentrations of methanol, ethanol, DMSO, glycerol, acetonitrile, and ethylene glycol led to the decrease of enzyme

activity of *S/LPMO14A* (Figure 3E). Among them, DMSO and ethylene glycol had the greatest effect on the activity of AA14 enzyme. Additionally, with the increase of organic solvent concentration, its inhibitory effect on *S/LPMO14A* activity was more obvious. After adding 40% ethanol, DMSO, and ethylene glycol, the enzyme activity of *S/LPMO14A* decreased to 13.5%, 17.8%, and 30.3% of the initial activity, respectively. This may be related to the fact that organic solvents affected various interactions within enzyme protein molecules or the ability of enzyme protein molecules to bind water, resulting in a loss of enzyme activity [31]. However, glycerol and acetonitrile had no obvious inhibitory effect on *S/LPMO14A* activity. When *S/LPMO14A* was incubated in different concentrations of organic solvent, its residual enzyme activity decreased to varying degrees (Figure 3F). Compared with 10% of organic solvent, 40% of organic solvent had a greater effect on *S/LPMO14A* enzyme stability. Among them, *S/LPMO14A* showed the best stability in glycerol and retained more than 84% of the initial enzyme activity after incubation of 40% of glycerol. It could be related to the fact that glycerol can protect proteins from a loss of activity as a commonly protective agent for enzyme proteins [32].

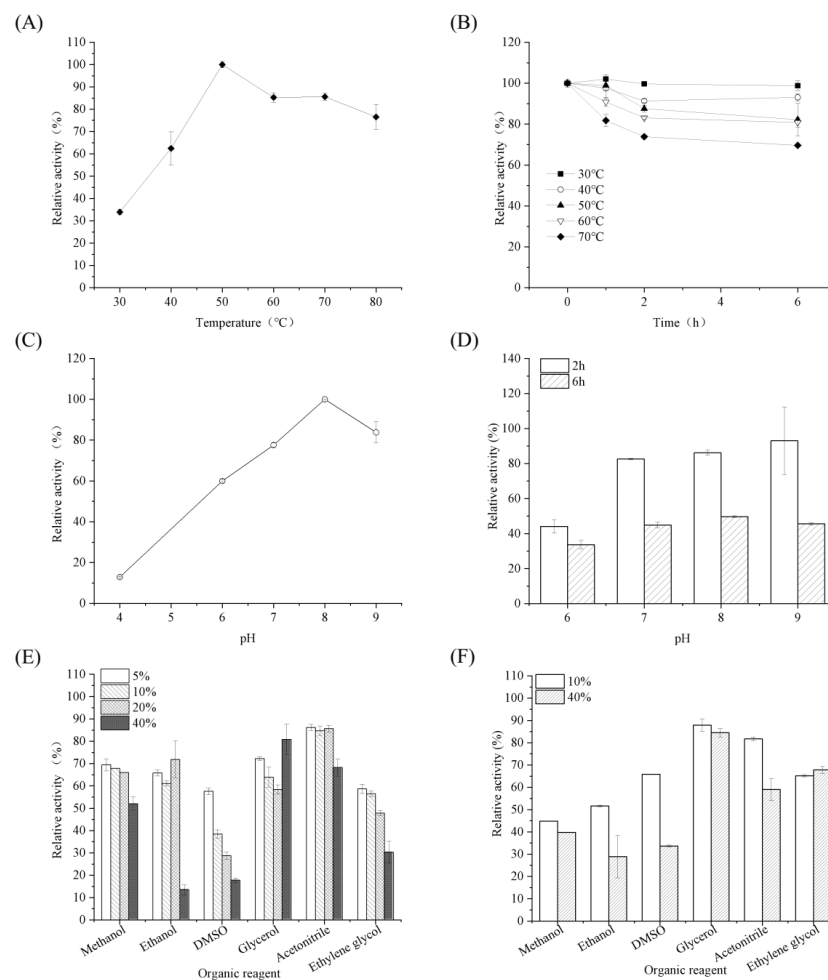


Figure 3. Enzymatic properties of *S/LPMO14A*. (A,B) are the effects of temperature on the activity and stability of *S/LPMO14A*, the reaction was carried out in 100 mM pH 8.0 Tris-HCl buffer and the reaction mixture contained 1 mM DMP, 2 μ M *S/LPMO14A*, and 100 μ M H₂O₂. (C,D) are the effects of pH on the activity and stability of *S/LPMO14A*. (E,F) are the effects of organic solvents on the activity and stability of *S/LPMO14A*. The activity of *S/LPMO14A* was determined using DMP as the substrate, the highest enzyme activity of *S/LPMO14A* was set as 100% or the initial enzyme activity (1.4 U/L) of *S/LPMO14A* was set as 100%.

3.3. Polysaccharides Cleavage and the Synergy Assays for the Saccharification of Biomass

The acid-pretreated pine and the xylan-coated cellulose film were used as substrates to evaluate the *S/LPMO14A* activity as an enzyme cocktail additive for enhanced ligno-cellulose saccharification. After the treatment of acid-pretreated pine by *S/LPMO14A*, a series of oxidation products were detected by MALDI-TOF MS (Figure 4A). It produced many oligosaccharides and oxidized oligosaccharides (both C1-oxidation products or C4-oxidation products) with degrees of polymerization (DPs) of 6–8. The identification of oxidative products indicated that *S/LPMO14A* was active on acid-pretreated pine [14]. The surface of the acid-pretreated pine was observed by environmental scanning electron micrographs (ESEM) (Figure 4B–E). It can be seen that the surface of the raw acid-pretreated pine was relatively flat and smooth, while some cracks appeared on the surface of the acid-pretreated pine after *S/LPMO14A* treatment, and some fragment-like areas could be observed. It could be related that *S/LPMO14A* oxidized xylan-coated cellulose fibers in the acid-pretreated pine, causing the structure to be destroyed and become looser.

The synergy assays between *S/LPMO14A* and cellulase, xylanase for acid-pretreated pine saccharification, were further used to study the contribution of *S/LPMO14A* enzymes to the saccharification of biomass, respectively (Figure 4F,G). It was observed that the releasing glucose and xylose from the substrates by cellulase and xylanase, respectively, were significantly increased after the addition of *S/LPMO14A*. Compared with the saccharification efficiency of acid-pretreated pine treated with cellulase and xylanase alone, the concentration of glucose and xylose increased 1.16-fold and 1.26-fold by the synergy assays with *S/LPMO14A*, respectively. These results were similar to the report that the addition of AA14 to the CL847 *Trichoderma reesei* enzyme cocktail and xylanase led to the significant release of glucose in pretreated softwood and xylooligomers in birchwood cellulose [14].

Xylan-coated cellulose film as an efficient and valid tool was further used to investigate the enhanced enzymatic hydrolysis by *S/LPMO14A* (Figure 5). Figure 5A showed the xylan-coated cellulose film could be efficiently oxidized and generated a series of oxidation products with degrees of polymerization (DPs) of 6–8 after treatment by *S/LPMO14A*. The raw cellulose film and the xylan-coated cellulose film before and after *S/LPMO14A* treatment were observed by atomic force microscopy. It could be seen that the fiber structure of the cellulose film alone was clearly visible (Figure 5B), while the surface of the xylan-coated cellulose film became blurred, and the fiber structure was not clear (Figure 5C). Compared with the untreated xylan-coated cellulose film, the fiber structure of the xylan-coated cellulose film treated with *S/LPMO14A* did not change significantly. Interesting, the Rq value significantly increased for xylan-coated cellulose film treated with *S/LPMO14A* (38 nm) compared to 30 nm and 32 nm for cellulose films and xylan-coated cellulose films, respectively, indicating that *S/LPMO14A* could oxidize xylan in xylan-coated cellulose film and increase the surface roughness (Figure 5D). These results were consistent with those previously reported, showing oxidative cleavage of highly refractory xylan-coated cellulose fibers by the AA14 family [14]. In the presence of *S/LPMO14A*, the concentration of releasing glucose and xylose reached 1.54 mg/mL and 0.88 mg/mL, respectively, which were 29.4% and 35.4% higher than those with the addition of cellulase and xylanase alone (Figure 5E,F). These results indicated that *S/LPMO14A* could significantly promote the degradation of xylan-coated cellulose substrate by cellulase and xylanase.

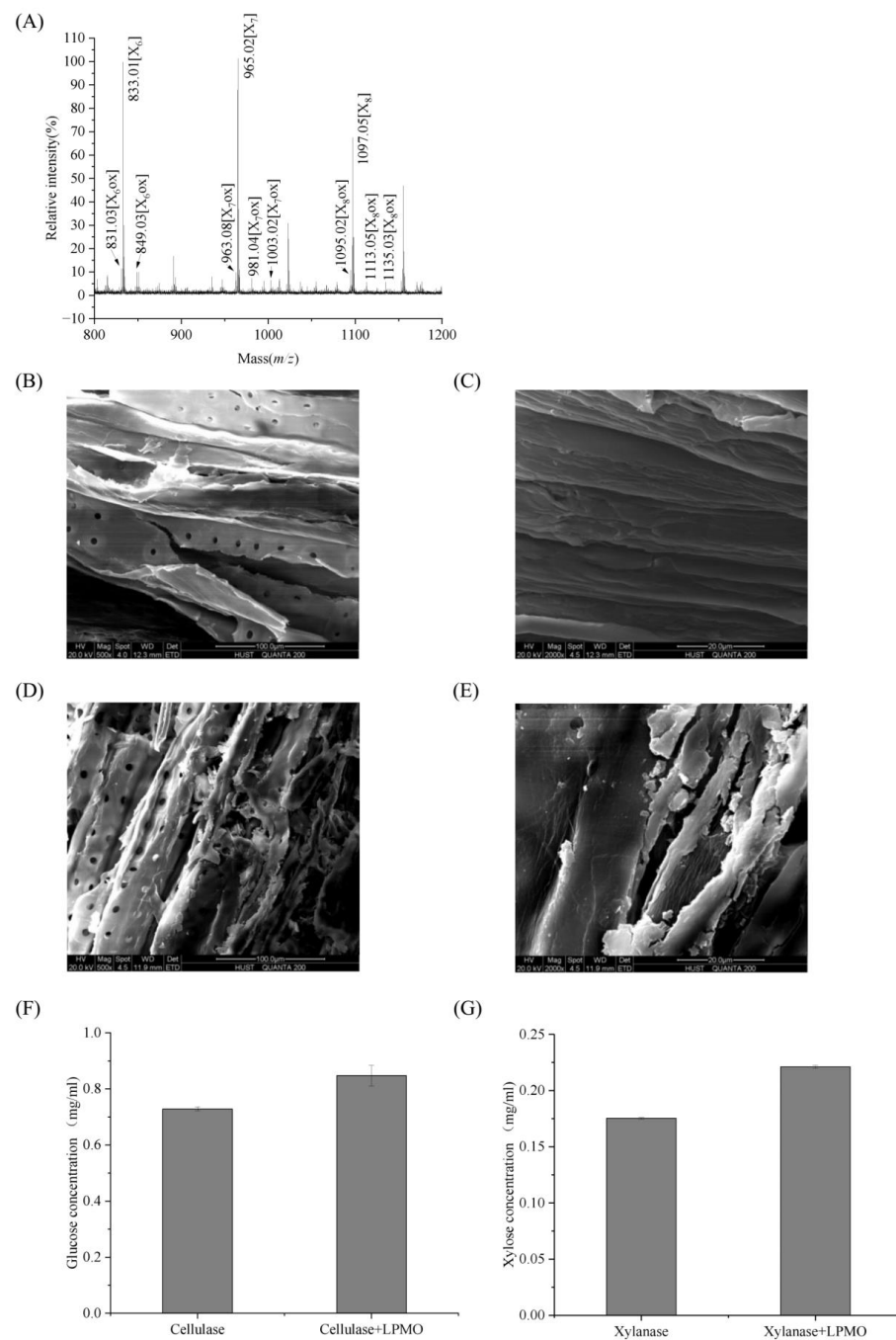


Figure 4. Polysaccharide cleavage and saccharification assays of acid-treated pine by *SILPMO14A*. (A) MALDI-TOF MS analysis of acid-treated pine oxidation products by *SILPMO14A*. The reaction mixture contained 1 μM *SILPMO14A*, 10 mg/mL substrate, 1 mM ascorbic acid. Additionally, it was incubated in 50 mM sodium acetate buffer (pH 5.0) at 50 $^{\circ}\text{C}$ for 48 h. The possible products in these clusters are native oligosaccharides (m/z 833.01, 965.02 and 1097.05) and C1-oxidative aldonic acids or C4-oxidative geminal diol (m/z 849.03, 981.04 and 1113.05), and C1-oxidised lactones or C4-oxidised ketoaldose (m/z 831.03, 963.08 and 1095.02), sodium salts of C1-oxidative aldonic acids (m/z 1003.02 and 1135.03). (B–E) Environmental scanning electron micrographs of acid-treated pine samples surface before (B,C) and after (D,E) treatment by *SILPMO14A*. The microscope magnification of (B,D) is 500 \times , the microscope magnification of (C,E) is 2000 \times . (F,G) Saccharification of acid pretreated pine by *SILPMO14A*. The reaction mixture contained 1 μM *SILPMO14A*, 60 U/(g substrates) cellulase or xylanase, 5 mg/mL substrate (acid pretreated pine), 1 mM ascorbic acid. Additionally, it was incubated in 50 mM sodium acetate buffer (pH 5.0) at 50 $^{\circ}\text{C}$ for 24 h.

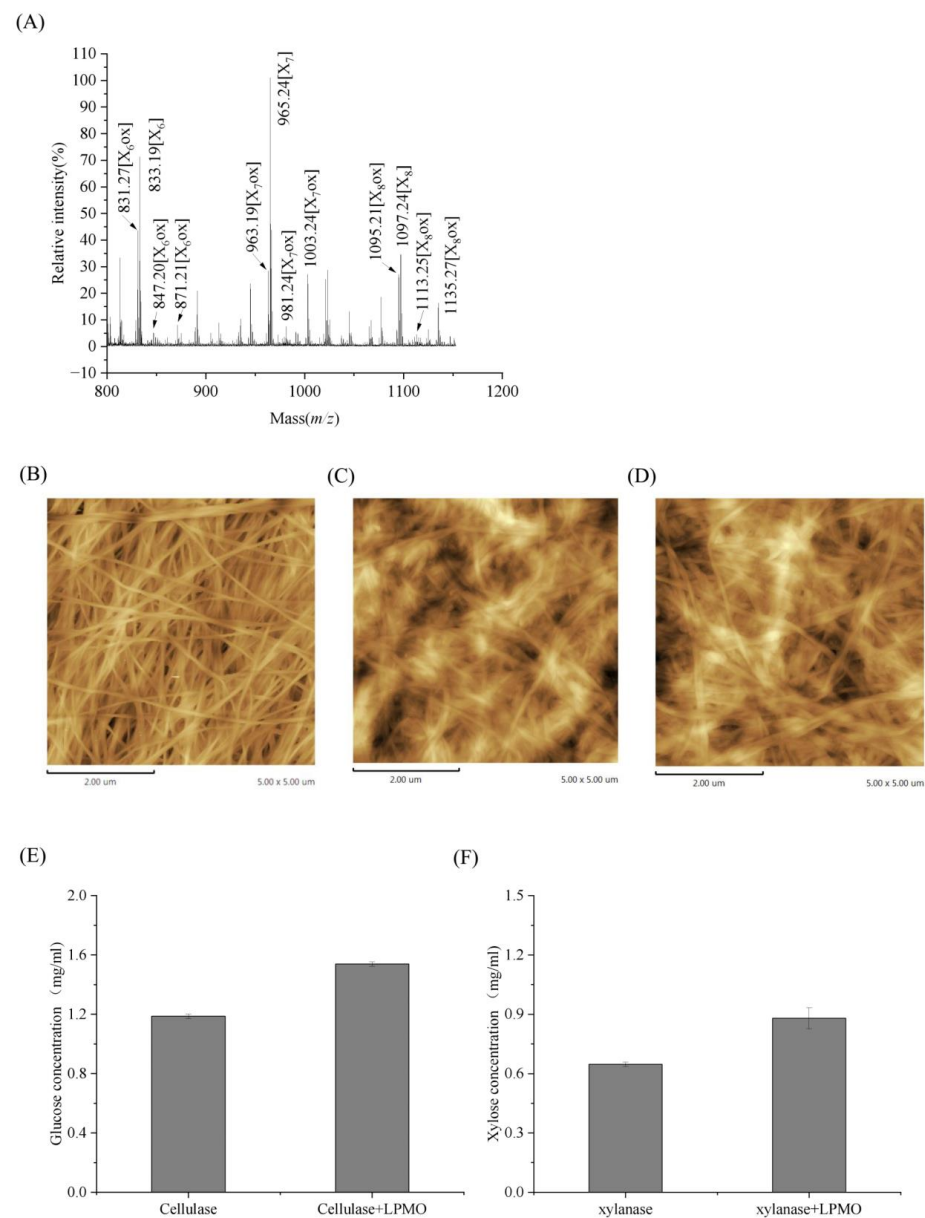


Figure 5. Polysaccharide cleavage and saccharification assays of xylan-coated cellulose film by SILPMO14A. (A) MALDI-TOF MS analysis of xylan-coated cellulose film oxidation products by SILPMO14A. The reaction mixture contained 1 μM SILPMO14A, 10 mg/mL substrate, 1 mM ascorbic acid. Additionally, it was incubated in 50 mM sodium acetate buffer (pH 5.0) at 50 $^{\circ}\text{C}$ for 48 h. The possible products in these clusters are native oligosaccharides (m/z 833.19, 965.24 and 1097.24) and C1-oxidative aldonic acids or C4-oxidative geminal diol (m/z 847.20, 981.24 and 1113.25), and C1-oxidised lactones or C4-oxidised ketoaldose (m/z 831.27, 963.19 and 1095.21), sodium salts of C1-oxidative aldonic acids (m/z 871.21, 1003.24 and 1135.27). (B–D) Microscopy analyses of enzyme-treated xylan-coated cellulose film. (B) AFM topography images of cellulose film; (C) AFM topography images of xylan-coated cellulose film; (D) AFM topography images of SILPMO14A-treated xylan-coated cellulose film. The Rq values measured for cellulose film (B), xylan-coated cellulose film (C), and SILPMO14A-treated xylan-coated cellulose film (D) were 30 nm, 32 nm, and 38 nm, respectively. (E,F) Saccharification of xylan-coated cellulose film by SILPMO14A. The reaction mixture contained 1 μM SILPMO14A, 60 U/(g substrates) cellulase or xylanase, 5 mg/mL substrate (xylan-coated cellulose film), 1 mM ascorbic acid. Additionally, it was incubated in 50 mM sodium acetate buffer (pH 5.0) at 50 $^{\circ}\text{C}$ for 24 h.

4. Conclusions

In this study, it was found that an AA14 gene (*SILPMO14A*, 468766) was upregulated in the early stage of lignocellulose degradation by *S. lacrymans* based on the transcriptomic analysis. The *SILPMO14A* was heterologously expressed and characterized. It was found to have maximum activity at 50 °C and pH 8.0. The *SILPMO14A* showed activity on acid-pretreated pine and xylan-coated cellulose substrates and could significantly increase the hydrolysis and saccharification of lignocellulose substrate. These results are of great significance for further understanding the role of LPMO on fungal degradation of lignocellulose and the construction of efficient enzyme cocktails in the field of biorefinery.

Supplementary Materials: The following supporting information can be downloaded at: <https://www.mdpi.com/article/10.3390/fermentation9060506/s1>, Table S1: Sequence of the *SILPMO14A*.

Author Contributions: Conceptualization, F.L. and H.Y.; data curation, F.L. and Y.L.; formal analysis, F.L., Y.L. and H.Z.; funding acquisition, F.L. and H.Y.; investigation, Y.L. and H.Y.; methodology, F.L., Y.L., H.Z. and X.L.; project administration, H.Y.; supervision, H.Y.; validation, H.Y.; visualization, Y.L.; writing—original draft, F.L. and Y.L.; writing—review and editing, H.Y. All authors have read and agreed to the published version of the manuscript.

Funding: This work was supported by the National Natural Science Foundation of China (31870083, 32000067) and the Scientific Research Foundation of Wuhan University of Science and Technology (No. 105005901).

Institutional Review Board Statement: Not applicable.

Informed Consent Statement: Not applicable.

Data Availability Statement: All data needed to evaluate the conclusions in the paper are present in the paper and/or the Supplementary Materials. Additional data related to this paper may be requested from the authors.

Acknowledgments: The authors thank the Centre of Analysis and Test of Huazhong University of Science for ESEM and AFM analysis and thank Technology and Core Facilities of Life Science (HUST).

Conflicts of Interest: The authors declare no conflict of interest.

References

1. Quinlan, R.J.; Sweeney, M.D.; Lo Leggio, L.; Otten, H.; Poulsen, J.C.N.; Johansen, K.S.; Krogh, K.; Jorgensen, C.I.; Tovborg, M.; Anthonsen, A.; et al. Insights into the oxidative degradation of cellulose by a copper metalloenzyme that exploits biomass components. *Proc. Natl. Acad. Sci. USA* **2011**, *108*, 15079–15084. [[CrossRef](#)] [[PubMed](#)]
2. Harris, P.V.; Welner, D.; McFarland, K.C.; Re, E.; Poulsen, J.C.N.; Brown, K.; Salbo, R.; Ding, H.S.; Vlasenko, E.; Merino, S.; et al. Stimulation of lignocellulosic biomass hydrolysis by proteins of glycoside hydrolase family 61: Structure and function of a large, enigmatic family. *Biochemistry* **2010**, *49*, 3305–3316. [[CrossRef](#)] [[PubMed](#)]
3. Kubicek, C.P.; Kubicek, E.M. Enzymatic deconstruction of plant biomass by fungal enzymes. *Curr. Opin. Chem. Biol.* **2016**, *35*, 51–57. [[CrossRef](#)] [[PubMed](#)]
4. Vandhana, T.M.; Reyre, J.L.; Sushmaa, D.; Berrin, J.G.; Bissaro, B.; Madhuprakash, J. On the expansion of biological functions of lytic polysaccharide monooxygenases. *New Phytol.* **2022**, *233*, 2380–2396. [[CrossRef](#)]
5. Tandrup, T.; Frandsen, K.E.H.; Johansen, K.S.; Berrin, J.G.; Lo Leggio, L. Recent insights into lytic polysaccharide monooxygenases (LPMOs). *Biochem. Soc. Trans.* **2018**, *46*, 1431–1447. [[CrossRef](#)]
6. Zhang, J.W.; Presley, G.N.; Hammel, K.E.; Ryu, J.S.; Menke, J.R.; Figueroa, M.; Hu, D.H.; Orr, G.; Schilling, J.S. Localizing gene regulation reveals a staggered wood decay mechanism for the brown rot fungus *Postia placenta*. *Proc. Natl. Acad. Sci. USA* **2016**, *113*, 10968–10973. [[CrossRef](#)]
7. Goodell, B.; Jellison, J.; Liu, J.; Daniel, G.; Paszczynski, A.; Fekete, F.; Krishnamurthy, S.; Jun, L.; Xu, G. Low molecular weight chelators and phenolic compounds isolated from wood decay fungi and their role in the fungal biodegradation of wood. *J. Biotechnol.* **1997**, *53*, 133–162. [[CrossRef](#)]
8. Ray, M.J.; Leak, D.J.; Spanu, P.D.; Murphy, R.J. Brown rot fungal early stage decay mechanism as a biological pretreatment for softwood biomass in biofuel production. *Biomass Bioenergy* **2010**, *34*, 1257–1262. [[CrossRef](#)]
9. Martinez, D.; Challacombe, J.; Morgenstern, I.; Hibbett, D.; Schmoll, M.; Kubicek, C.P.; Ferreira, P.; Ruiz-Duenas, F.J.; Martinez, A.T.; Kersten, P.; et al. Genome, transcriptome, and secretome analysis of wood decay fungus *Postia placenta* supports unique mechanisms of lignocellulose conversion. *Proc. Natl. Acad. Sci. USA* **2009**, *106*, 1954–1959. [[CrossRef](#)]

10. Hori, C.; Gaskell, J.; Igarashi, K.; Samejima, M.; Hibbett, D.; Henrissat, B.; Cullen, D. Genomewide analysis of polysaccharides degrading enzymes in 11 white- and brown-rot Polyporales provides insight into mechanisms of wood decay. *Mycologia* **2013**, *105*, 1412–1427. [[CrossRef](#)]
11. Floudas, D.; Binder, M.; Riley, R.; Barry, K.; Blanchette, R.A.; Henrissat, B.; Martinez, A.T.; Otilar, R.; Spatafora, J.W.; Yadav, J.S.; et al. The Paleozoic origin of enzymatic lignin decomposition reconstructed from 31 fungal genomes. *Science* **2012**, *336*, 1715–1719. [[CrossRef](#)] [[PubMed](#)]
12. Eastwood, D.C. The plant cell wall-decomposing machinery underlies the functional diversity of forest fungi. *Science* **2011**, *333*, 762–765. [[CrossRef](#)] [[PubMed](#)]
13. Kojima, Y.; Varnai, A.; Ishida, T.; Sunagawa, N.; Petrovic, D.M.; Igarashi, K.; Jellison, J.; Goodell, B.; Alfredsen, G.; Westereng, B.; et al. A lytic polysaccharide monoxygenase with broad xyloglucan specificity from the brown-rot fungus *Gloeophyllum trabeum* and its action on cellulose-xyloglucan complexes. *Appl. Environ. Microbiol.* **2016**, *82*, 6557–6572. [[CrossRef](#)] [[PubMed](#)]
14. Couturier, M.; Ladeveze, S.; Sulzenbacher, G.; Ciano, L.; Fanuel, M.; Moreau, C.; Villares, A.; Cathala, B.; Chaspoul, F.; Frandsen, K.E.; et al. Lytic xylan oxidases from wood-decay fungi unlock biomass degradation. *Nat. Chem. Biol.* **2018**, *14*, 306–310. [[CrossRef](#)]
15. Zerva, A.; Pentari, C.; Grisel, S.; Berrin, J.G.; Topakas, E. A new synergistic relationship between xylan-active LPMO and xylobiohydrolase to tackle recalcitrant xylan. *Biotechnol. Biofuels* **2020**, *13*, 142. [[CrossRef](#)]
16. Mahajan, R.; Hudson, B.S.; Sharma, D.; Kolte, V.; Sharma, G.; Goel, G. Transcriptome analysis of *Podoscypha petalodes* strain GGF6 reveals the diversity of proteins involved in lignocellulose degradation and ligninolytic function. *Indian J. Microbiol.* **2022**, *62*, 569–582. [[CrossRef](#)]
17. Forsberg, Z.; Vaaje-Kolstad, G.; Westereng, B.; Bunaes, A.C.; Stenstrom, Y.; MacKenzie, A.; Sorlie, M.; Horn, S.J.; Eijsink, V.G.H. Cleavage of cellulose by a CBM33 protein. *Protein Sci.* **2011**, *20*, 1479–1483. [[CrossRef](#)]
18. Li, F.; Zhao, H.L.; Liu, Y.X.; Zhang, J.Q.; Yu, H.B. Chitin biodegradation by lytic polysaccharide monoxygenases from *Streptomyces coelicolor* in vitro and in vivo. *Int. J. Mol. Sci.* **2023**, *24*, 275. [[CrossRef](#)]
19. Loose, J.S.M.; Forsberg, Z.; Fraaije, M.W.; Eijsink, V.G.H.; Vaaje-Kolstad, G. A rapid quantitative activity assay shows that the *Vibrio cholerae* colonization factor GbpA is an active lytic polysaccharide monoxygenase. *FEBS Lett.* **2014**, *588*, 3435–3440. [[CrossRef](#)]
20. Kittl, R.; Kracher, D.; Burgstaller, D.; Haltrich, D.; Ludwig, R. Production of four *Neurospora crassa* lytic polysaccharide monoxygenases in *Pichia pastoris* monitored by a fluorimetric assay. *Biotechnol. Biofuels* **2012**, *5*, 79. [[CrossRef](#)]
21. Breslmayr, E.; Hanzek, M.; Hanrahan, A.; Leitner, C.; Kittl, R.; Santek, B.; Oostenbrink, C.; Ludwig, R. A fast and sensitive activity assay for lytic polysaccharide monoxygenase. *Biotechnol. Biofuels* **2018**, *11*, 79. [[CrossRef](#)]
22. Siqueira, G.; Varnai, A.; Ferraz, A.; Milagres, A.M.F. Enhancement of cellulose hydrolysis in sugarcane bagasse by the selective removal of lignin with sodium chlorite. *Appl. Energy* **2013**, *102*, 399–402. [[CrossRef](#)]
23. Ni, H.X.; Li, M.J.; Li, F.; Wang, L.; Xie, S.X.; Zhang, X.Y.; Yu, H.B. In-situ lignin drives lytic polysaccharide monoxygenases to enhance enzymatic saccharification. *Int. J. Biol. Macromol.* **2020**, *161*, 308–314. [[CrossRef](#)] [[PubMed](#)]
24. Li, F.; Ma, F.Y.; Zhao, H.L.; Zhang, S.; Wang, L.; Zhang, X.Y.; Yu, H.B. A lytic polysaccharide monoxygenase from a white-rot fungus drives the degradation of lignin by a versatile peroxidase. *Appl. Environ. Microbiol.* **2019**, *85*, e02803–e02818. [[CrossRef](#)] [[PubMed](#)]
25. Li, F.; Sun, X.J.; Yu, W.; Shi, C.C.; Zhang, X.Y.; Yu, H.B.; Ma, F. Enhanced konjac glucomannan hydrolysis by lytic polysaccharide monoxygenases and generating prebiotic oligosaccharides. *Carbohydr. Polym.* **2021**, *253*, 117241. [[CrossRef](#)] [[PubMed](#)]
26. Brenelli, L.; Squina, F.M.; Felby, C.; Cannella, D. Laccase-derived lignin compounds boost cellulose oxidative enzymes AA9. *Biotechnol. Biofuels* **2018**, *11*, 10. [[CrossRef](#)] [[PubMed](#)]
27. Zhu, Y.; Plaza, N.; Kojima, Y.; Yoshida, M.; Zhang, J.W.; Jellison, J.; Pingali, S.V.; O'Neill, H.; Goodell, B. Nanostructural analysis of enzymatic and non-enzymatic brown rot fungal deconstruction of the lignocellulose cell wall. *Front. Microbiol.* **2020**, *11*, 1389. [[CrossRef](#)] [[PubMed](#)]
28. Manavalan, T.; Stepnov, A.A.; Hegnar, O.A.; Eijsink, V.G.H. Sugar oxidoreductases and LPMOs—two sides of the same polysaccharide degradation story? *Carbohydr. Res.* **2021**, *505*, 108350. [[CrossRef](#)]
29. Kracher, D.; Scheiblbrandner, S.; Felice, A.K.G.; Breslmayr, E.; Preims, M.; Ludwicka, K.; Haltrich, D.; Eijsink, V.G.H.; Ludwig, R. Extracellular electron transfer systems fuel cellulose oxidative degradation. *Science* **2016**, *352*, 1098–1101. [[CrossRef](#)]
30. Bissaro, B.; Rohr, A.K.; Muller, G.; Chylenski, P.; Skaugen, M.; Forsberg, Z.; Horn, S.J.; Vaaje-Kolstad, G.; Eijsink, V.G.H. Oxidative cleavage of polysaccharides by monocopper enzymes depends on H₂O₂. *Nat. Chem. Biol.* **2017**, *13*, 1123–1128. [[CrossRef](#)]
31. Serdakowski, A.L.; Dordick, J.S. Enzyme activation for organic solvents made easy. *Trends Biotechnol.* **2008**, *26*, 48–54. [[CrossRef](#)] [[PubMed](#)]
32. Gangadhara; Kumar, P.; Prakash, V. Influence of polyols on the stability and kinetic parameters of invertase from *Candida utilis*: Correlation with the conformational stability and activity. *Protein J.* **2008**, *27*, 440–449. [[CrossRef](#)] [[PubMed](#)]

Disclaimer/Publisher's Note: The statements, opinions and data contained in all publications are solely those of the individual author(s) and contributor(s) and not of MDPI and/or the editor(s). MDPI and/or the editor(s) disclaim responsibility for any injury to people or property resulting from any ideas, methods, instructions or products referred to in the content.